Proton capture by ^{15}N above the giant dipole resonance

M. Anghinolfi, P. Corvisiero, G. Ricco, M. Sanzone, M. Taiuti, and A. Zucchiatti
Istituto di Scienze Fisiche dell'Università di Genova
and Istituto Nazionale di Fisica Nucleare—Sezione di Genova, 5-16132 Genova, Italy
(Received 2 March 1983)

The proton capture cross sections to the ground and excited states of ^{16}O have been measured at several angles in the proton energy interval between 18 and 40 MeV. The ground state angular distribution, which shows a significant $E1$-$E2$ interference effect above 40 MeV, results in reasonable agreement with semidirect capture calculations. Transitions to final bound and unbound 1p-1h states in ^{16}O having a dominant $1p_{1/2}^{-1}$ hole have also been measured. Resonances built on these residual states have been systematically observed above $E_p = 20$ MeV; the possible interpretation of these states as giant dipole resonances built on excited states is discussed.

[NUCLEAR REACTIONS ^{15}N(p,γ_x)^{16}O. Measured $\sigma(\theta)$ at seven angles and proton energies between 18 and 40 MeV; deduced A_0 and a_k coefficients. Enriched gas target, anticoincidence NaI detector.]

INTRODUCTION

Radiative proton capture experiments have proven to be, at excitation energies above the giant dipole resonance (GDR), a successful method of investigation of nuclear structure. The differential ground state (g.s.) capture cross section should be, at intermediate energies, fairly sensitive to correlation effects in the g.s. wave function,[1,2] while the excited state capture cross section recently revealed new and rather unexpected excitation mechanisms. In the ^{11}B(p,γ_x)^{12}C reaction different experiments[3–5] have reported dominant transitions to residual levels at excitation energies E_x as high as 19 MeV in ^{12}C. Theoretical analysis[6,7] in terms of a direct capture mechanism is unable to reproduce the main features of the experimental data, and semidirect capture to high lying states is probably required.[6] Each experimental p,γ_x cross section shows, in fact, a complex resonant structure[4,5] as a function of the incident proton energy: The centroid energy

$$\langle E_r \rangle = \int \omega \sigma_{p\gamma_x}(\omega) d\omega$$

systematically lies 20—22 MeV above the residual state energy E_x.[5,8] Moreover, the analysis of differential cross sections reports dominant $E1$ absorption with non-

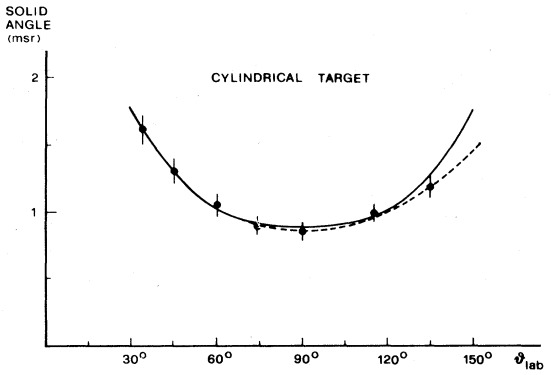

FIG. 1. Average solid angle for our 40 cm long cylindrical gas target measured, as a function of detection angle, as described in the text. The full curve is the result of a Monte Carlo calculation performed in the experimental geometry, and the dotted curve is a numerical fit of the data points.

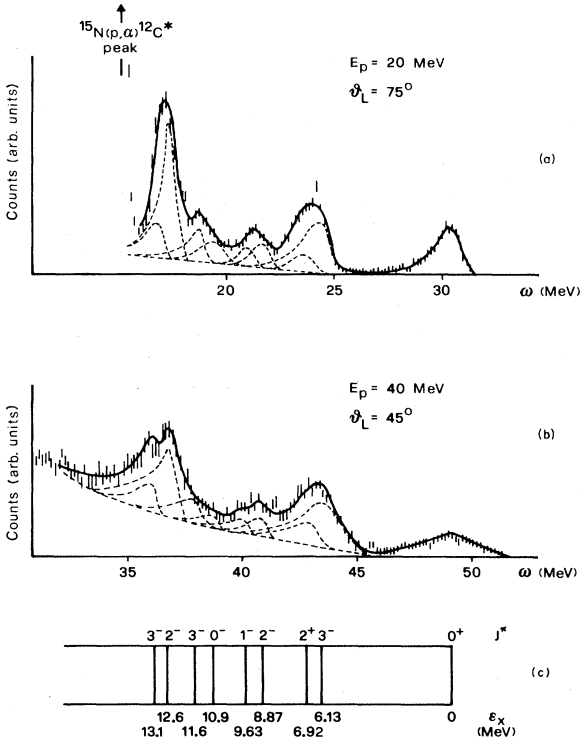

FIG. 2. Capture photon spectra (a) and (b) to the 1p-1h ($1p_{1/2}^{-1}$) residual states of ^{16}O. (c) The continuous curve is the fit obtained as the sum of nine response functions plus a continuous background.

TABLE I. Experimental differential cross section $d\sigma/d\Omega_{\text{c.m.}}$ for the (p,γ_0) channel (in μb/sr). E_p is the proton energy in the laboratory system and $\theta_{\text{c.m.}}$ is the photon emission angle in the c.m. system.

$\theta_{\text{c.m.}}$ \ E_p	18.1	19.7	20.7	21.7	23.8	25.8	27.8	31.8	35.8	39.8
34.5±2	1.26±0.06	0.72±0.04	0.79±0.04	0.71±0.04	0.63±0.03	0.57±0.03	0.47±0.02	0.30 ±0.02	0.20±0.01	0.20 ±0.01
45.6±2	1.62±0.10	0.95±0.06	1.03±0.06	0.94±0.06	0.70±0.04	0.71±0.04	0.49±0.03	0.37 ±0.02	0.27±0.01	0.24 ±0.015
60.7±2	1.88±0.14	1.06±0.07	1.13±0.07	0.88±0.06	0.86±0.06	0.73±0.05	0.53±0.03	0.35 ±0.02	0.28±0.02	0.22 ±0.015
75.8±2	2.01±0.15	1.11±0.08	1.15±0.09	1.03±0.10	0.84±0.06	0.71±0.05	0.54±0.04	0.30 ±0.02	0.22±0.02	0.20 ±0.02
90.8±2	1.95±0.15	1.06±0.08	0.94±0.07	0.89±0.07	0.76±0.06	0.58±0.04	0.39±0.03	0.23 ±0.02	0.14±0.01	0.11 ±0.01
115.8±2	1.42±0.10	0.59±0.04	0.66±0.05	0.50±0.03	0.37±0.03	0.38±0.03	0.23±0.02	0.16 ±0.01	0.07±0.006	0.035±0.004
135.6±2	0.90±0.05	0.38±0.02	0.38±0.03	0.32±0.02	0.25±0.01	0.21±0.01	0.14±0.01	0.059±0.005	0.03±0.003	0.014±0.002

negligible $E2$ interference terms.[5] All these features support the interpretation of the observed structures as giant dipole resonances built on the excited 1p-1h states of ^{12}C. A similar interpretation was recently proposed[9] for the ^{27}Al(p,γ_x)^{28}Si cross sections, even though the higher residual level density in ^{28}Si makes the data interpretation more difficult. Since these new $E1$ giant resonances seem to be rather systematic, at least in closed shell or subshell nuclei, their observation in ^{16}O would provide important confirmation.

In this work the differential ^{15}N(p,γ)^{16}O cross section has been measured at seven detection angles in the proton energy range between 20 and 40 MeV.

EXPERIMENTAL SETUP AND DATA ANALYSIS

The proton beam from the 45 MeV cyclotron of Milano University was focused on a 99% pure ^{15}N gas target and monitored by a Faraday cup. Capture photons were detected by a 24 cm$\times$32 cm cylindrical NaI detector surrounded by a 9 cm thick Ne110 anticoincidence shield, the whole system being movable between 35° and 135°. The detection solid angle, 4 msr for a point target, was defined by a distributed system of lead and iron collimators. Capture photon pulses were selected through a cascade of anticoincidence gates: Pileup pulses were rejected above and below the energy threshold, cosmic rays and energy escapes by the NE110 shielding, and neutrons by time of flight discrimination.[5]

The scintillators and the relevant electronics are discussed in detail in Ref. 10. The gas target was a sealed 40 cm long aluminum cylinder filled with 1.3 atm ^{15}N gas for a total thickness of 64 mg/cm^2, corresponding to an energy spread of about $\pm$0.70%. The gas pressure, continuously monitored by a 3% precision manometer, was constant during a whole week run. The entrance and exit windows, each made of a 13 mg/cm^2 Mylar foil, gave negligible background due to the small detection solid angle at the target edges.

The effect of the extended target on the solid angle was determined by measuring the yield of the 15.11 MeV p,p'γ peak from our target, filled with 1.3 atm CH_4 gas, and from an equally thick solid polyethylene target. The experimental results are displayed in Fig. 1. The dotted line is a fit of the data, while the continuous curve is the result of a Monte Carlo calculation. The slight difference at large angle is probably due to a possible system misalignment at backward angles; the fitted curve has therefore been chosen for the data analysis.

The capture photon spectrum shows, besides the ground state transition, several peaks (Fig. 2) corresponding to p,γ_x transitions to final 1p-1h ^{16}O states at 6.1+6.9, 8.9+9.6, 11.6, and 12.6+13.1 MeV, all having a dominant $(1p_{1/2})^{-1}$ hole configuration. The errors on the absolute cross sections reported in Figs. 3—8 result from the contribution of counting statistics ($\sim$3%), uncertainties on the detection solid angle (4%), and target thickness (3%). The evaluation of the single peak area from the overlapped spectra requires a detailed knowledge of the detector response function, since the results will depend upon the assumed γ line shape. In this work the following procedure was adopted: The "intrinsic" response function

$F(\omega,E_\gamma)$ (Ref. 12) and efficiency of our anticoincidence detector

$$\text{eff}(E_\gamma)=\int F(\omega,E_\gamma)d\omega$$

were computed by a Monte Carlo (MC) code[11] already tested with monochromatic photon data in the same energy interval. The line shape $S(\omega,E_\gamma)$ has been assumed as the convolution of the intrinsic MC detector response with a Gaussian function, which simulates statistical fluctuations in light collection and amplification:

$$S(\omega,E_\gamma)=\int F(\omega',E_\gamma)G\left[\frac{\omega-\omega'}{\sigma_s}\right]d\omega' .$$

The statistical variance $\sigma_s(E_\gamma)$ has been determined as a function of the incident photon energy by optimizing the observed FWHM on the well-resolved ^{11}B(p,γ_0)^{12}C and ^{12}C(p,γ_0)^{13}N transitions.[12] The capture photon spectra (Fig. 2) were then fitted, using the iterative procedure described in Ref. 5, as the sum of nine peaks plus a continuous background. The peak energy is given, for each observed residual state energy ϵ_x and detection angle θ, by

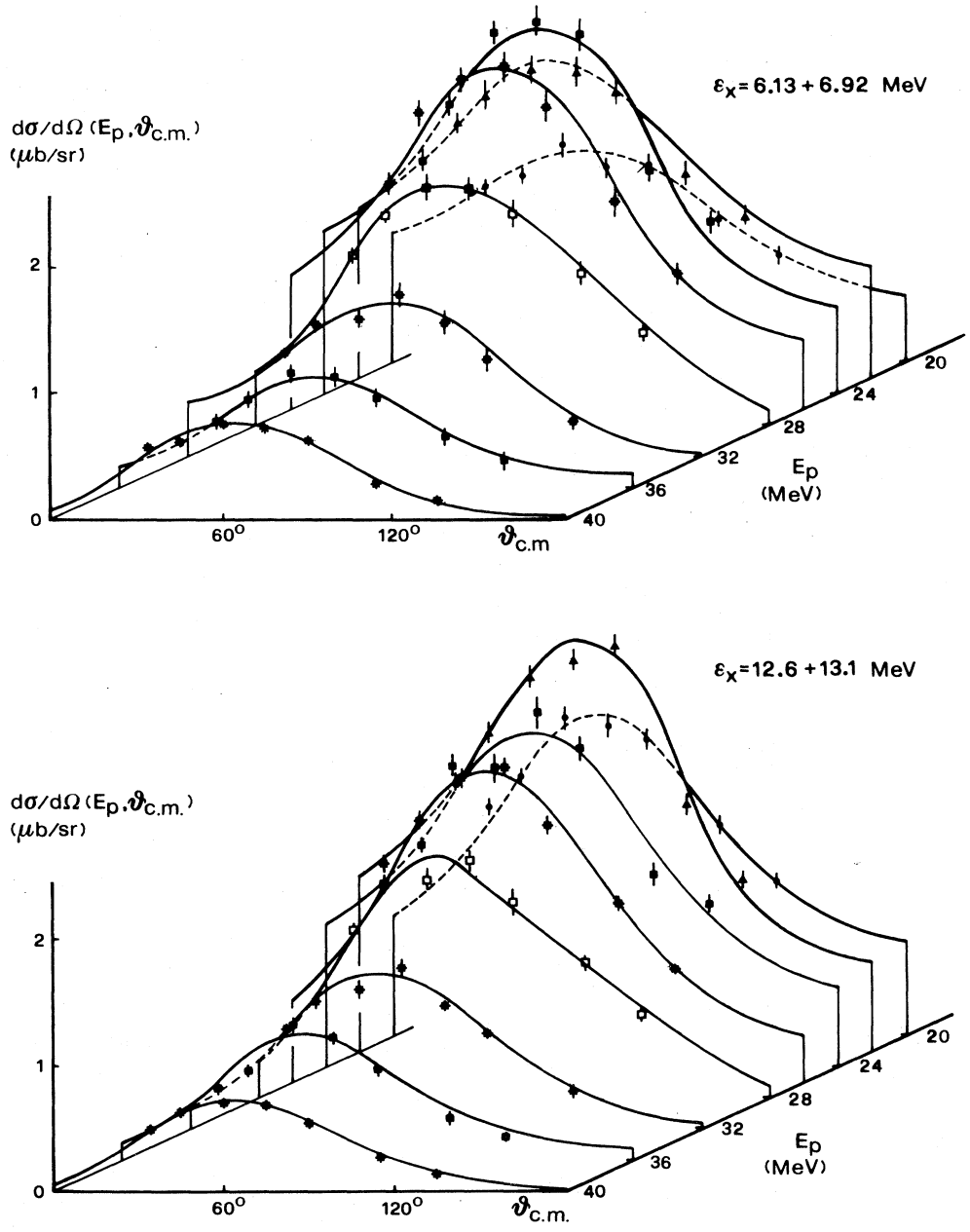

FIG. 3. Differential c.m. cross sections for proton capture to groups of final states of excitation energy ϵ_x in ^{16}O. The curves are fits performed using four Legendre polynomial expansion.

the approximate relation

$$E_{\text{peak}} \simeq 0.99 E_\gamma ,$$

$$E_\gamma = \frac{T_p(m_A - m_p) + B(m_A + T_p)}{B - \cos\theta \sqrt{T_p(T_p + 2m_p)} + m_A T_p} ,$$

where m_A is the mass of the final nucleus, m_p is the proton mass, and

$$B = m_p + m_{A-1} - m_A - \epsilon_x ,$$

where E_γ is the emitted photon energy and the difference

$$\delta = E_{\text{peak}} - E_\gamma \simeq -0.01 E_\gamma$$

is due to energy escape. The total peak width is also fixed by the convolution of the computed intrinsic σ_{MC} and statistical σ_s contributions. For each peak in Fig. 2 the fit is determined by the area A_i and by two parameters for the underlying linear background.[5] A nonzero background, generally more relevant at forward angles and higher proton energies, is systematically required to optimize the observed line shape to the response function $S(\omega, E_\gamma)$ and to get continuity with the lower energy part of the measured spectra (Fig. 2).

DISCUSSION

The experimental center of mass cross section

$$\frac{d\sigma}{d\Omega}(E_p, \theta)$$

has been reported, as a function of the incident proton energy E_p and center of mass angle $\theta_{c.m.}$, in Table I for the ground state p,γ_0 transition and in Fig. 3 for the most important p,γ_x transitions. The ground state cross section shows a forward peaking, due to $(E1,E2)$ interference (more pronounced at the higher excitation energies) and a smooth energy dependence. The p,γ_x data exhibit a more spread out angular distribution and a resonant behavior. If the well-known expansion

$$\frac{d\sigma}{d\Omega_{c.m.}} = A_0 \left[1 + \sum_{k=1}^{2L} a_k P_k(\cos\theta_{c.m.}) \right] \quad (1)$$

is used and the sum is truncated to multipolarity order $EL \leq E2$ and $ML \leq M1$, the a_2 and a_1 coefficients are related to the main dipole transition and its interference terms with the other multipoles $(E2,M1)$, while a_4 and a_3 are due to the quadrupole strength and to $(E1,E2)$ interference, respectively. Non-negligible electric octupole $E3$ absorption would extend expansion (1) to include the $a_5(E2,E3)$ and $a_6(|E3|^2)$ coefficients; a further contribution should arise in this case to a_2 and a_4 from $(E1,E3)$ interference and to a_1 and a_3 from $(E2,E3)$ interference.[15] The extension to $k=5$ does not improve the fits in the angular range of this experiment, but is required in order to reproduce the strong forward peaking of (γ,p_0) data above 60 MeV.[13] The ground state cross section has been computed by the Bologna group in the framework of self-consistent RPA calculations[14]: The single particle energies, the bound and scattering wave functions, and the p-h interaction are consistently obtained from phenomenological forces. In the calculation, limited to $E1$ and $E2$ transitions only, long range correlations arise from the residual Skyrme 3 interaction, and meson exchange currents have been accounted for by the use of the Siegert theorem. Quadrupole absorption is predicted above the GDR with a high isoscalar peak at about 21 MeV and a broadly distributed isovector strength at higher energies.[14] This quadrupole strength is responsible, mainly through $(E1,E2)$ interference, for the behavior of the theoretical a_1, a_3, and a_4 coefficients[16] reported in Fig. 4, the change of slope around 45 MeV being determined by the isovector component. The overall agreement of the theoretical coefficients with our experimental data (Fig. 4) is fairly good, at least above the GDR even if the $E2$ strength seems to be shifted a few MeV upwards with respect to the RPA predictions. This calculation does not include the tensor component in the Skyrme interaction and multipolarity order higher than $E2$; since the relative importance of these effects is expected to increase with the photon energy, the observed deviation of the RPA prediction from the experimental data above 60 MeV is not surprising.

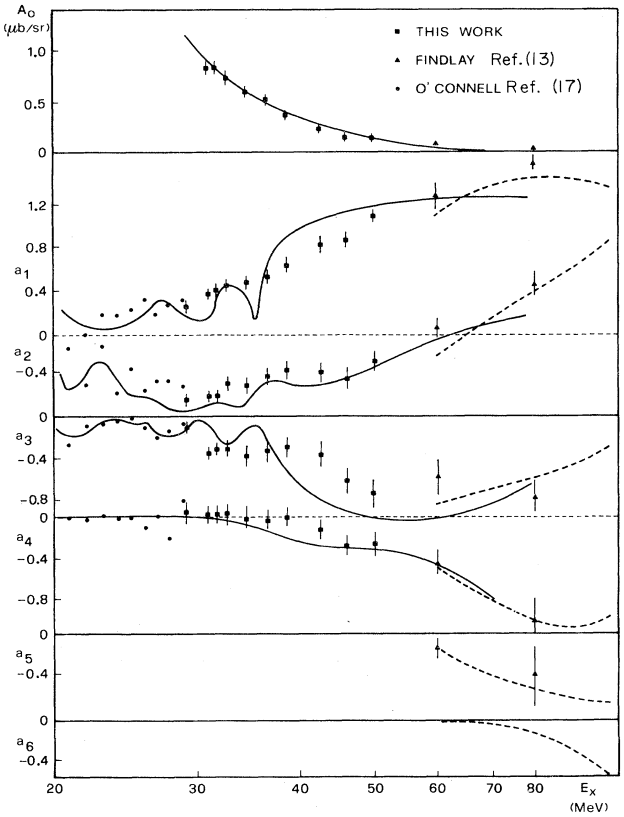

FIG. 4. Legendre expansion coefficients of the quoted pγ_0 and γp_0 cross sections. The continuous curve and the dotted curve are the results of a self-consistent RPA calculation (Ref. 14) and of a semidirect interaction model (Ref. 2), respectively.

At higher energies a direct plus semidirect capture model using phenomenological single particle wave functions has been developed by the Bochum group[2]: In this approach initial and final state correlations (CORR) have been introduced in the shell model wave functions (SM) through a Yukawa type of interaction, and meson exchange currents (MEC) have been included by the use of

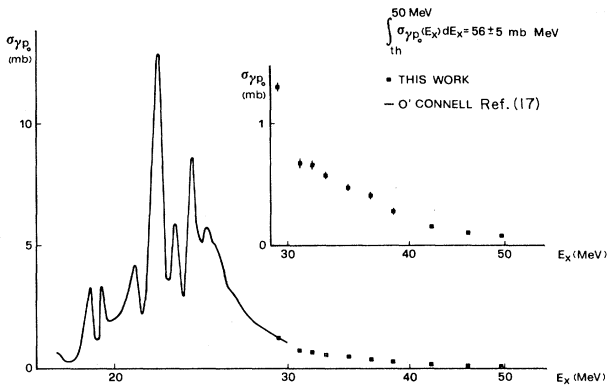

FIG. 5. Ground state photodisintegration cross section γp_0 as a function of the incident photon energy E_x. The integrated cross section has been evaluated down to the threshold using data of Refs. (17) and (27).

effective two body operators. Tensor correlations, which are known to enhance[23] photonuclear absorption at higher energies, have been indirectly accounted for by renormalization of the residual interaction strength in order to fit the dipole sum rule. The angular distribution coefficients a_k, not explicitly computed in Ref. 2, can be evaluated[18] expanding the theoretical (SM + CORR + MEC) differential cross sections according to Eq. (1) up to $L=3$ (the dotted curves in Fig. 4). Reasonable agreement with experimental (γ,p_0) data is also obtained in the 60—100 MeV range by simple direct reaction models[21]: The cross section is, however, strongly dependent upon the assumed single particle potential, and the magnitude of the (γ,n) cross section cannot be reproduced without the use of effective charges.[22] The (γ,p_0) cross section, obtained through detailed balance, is plotted in Fig. 5 together with the experimental data of Ref. 17. The integrated cross section up to 100 MeV is 57.8±5. mb MeV (the contribution above 30 MeV amounts to 8.0 mb MeV); this figure corresponds to 24% of the classical sum rule and to 18% of the absorption cross section integrated up to 140 MeV as evaluated in Ref. 24.

Systematic measurements of the differential $^{16}O(\gamma,n_0)$ cross section have been performed up to 45 MeV.[19] The reported Legendre polynomial expansion coefficients a_{0n}, a_{2n}, and a_{3n} are, in the 30—45 MeV energy interval, in fair agreement with the corresponding a_k coefficients of Fig. 4; a_{1n} is lower for neutrons and a_{4n} is fairly constant around 0.2—0.3. These values lead to an $E2$ cross section[19] exhausting approximately 68% of the isovector EWSR between 25 and 40 MeV. RPA calculations[26] reproduce fairly well the general trend of these data and the cross section magnitude, but predict[14] considerably lower $E2$ strength, and therefore smaller a_{4n}, below 35 MeV. Also the (γ,p_0) cross section gives small negative a_{4p} in the -0.1—0.0 range for $E_x=25$—40 MeV, suggesting small proton isovector $E2$ strength in this energy range, in closer agreement with RPA predictions.

The success of the semidirect interaction models in reproducing the (γ,p_0) and, to some extent the (γ,n_0) cross sections up to 100 MeV, confirms the importance of long range correlations in the photodisintegration of light nuclei above the giant dipole resonance region.

The same expansion (1) has been applied to the experimental (p,γ_x) data; in this case the larger uniformity of the experimental angular distribution increases the ambiguity in the evaluation of the a_k coefficients. Since our data include angles from 35° to 135° only, further constraints have been imposed to the fit:

$$\frac{d\sigma}{d\Omega} \geq 0, \quad \left.\frac{d\sigma}{d\Omega}\right|_{180°} \leq \left.\frac{d\sigma}{d\Omega}\right|_{150°} \leq \left.\frac{d\sigma}{d\Omega}\right|_{125°} .$$

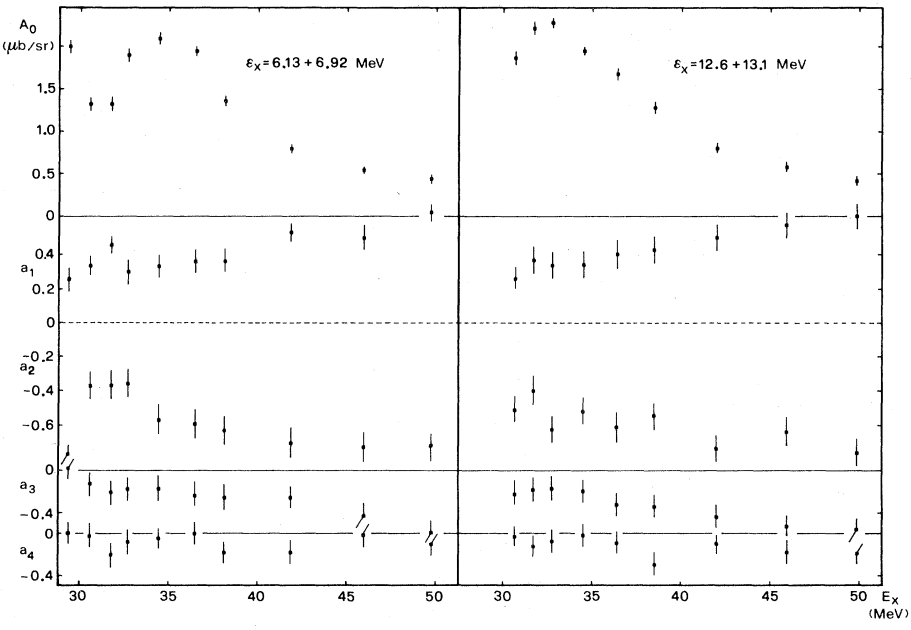

FIG. 6. Legendre expansion coefficients corresponding to the curves of Fig. 3.

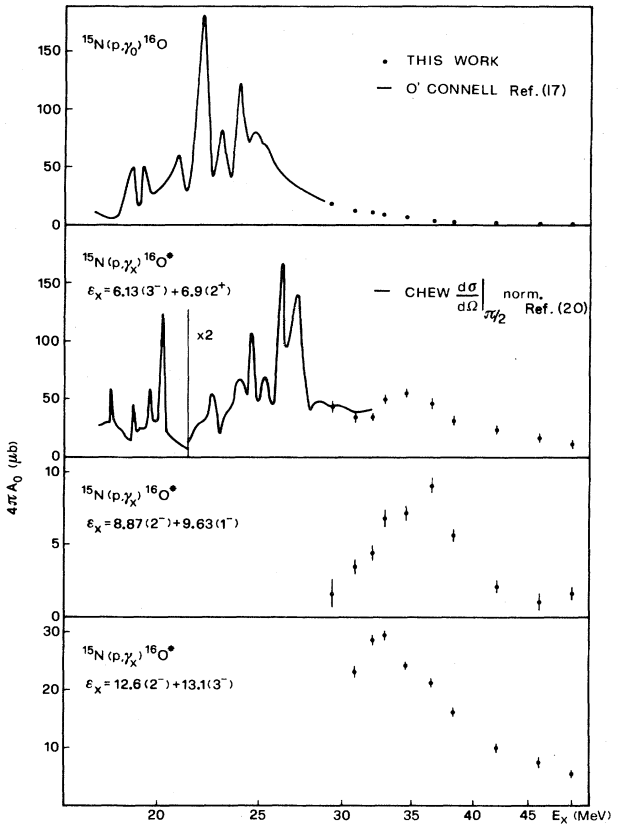

FIG. 7. The cross section $\sigma_t = 4\pi A_0$ as a function of the excitation energy E_x for p,γ_x transitions to groups of residual states in ^{16}O of energy ϵ_x.

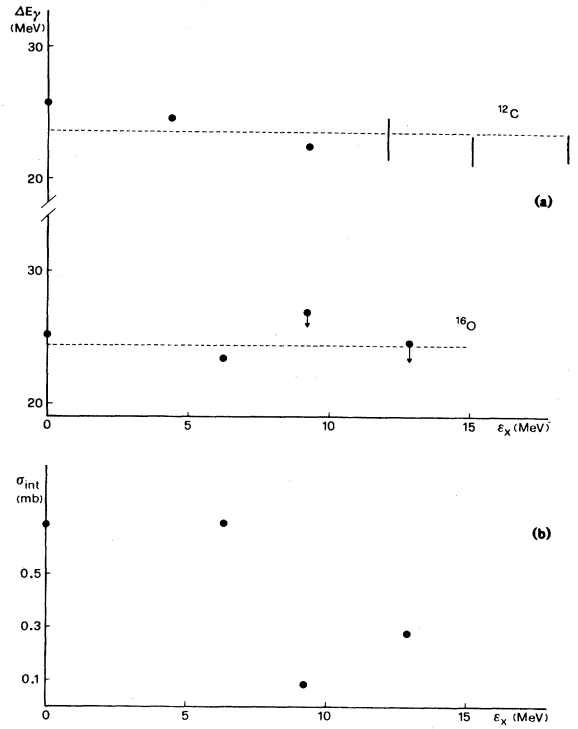

FIG. 8. (a) Energy shift $\Delta E_\gamma = \langle E \rangle - \epsilon_x$ of the centroid excitation energy $\langle E \rangle$ as a function of the residual energy ϵ_x in ^{12}C (Ref. 8) and ^{16}O. Arrows and error bars report the uncertainty due to the lack of low energy data. (b) Integrated capture cross section, above 17.5 MeV for pγ_0 and pγ_{1+2} and above 30 MeV for the remaining transitions, for the various residual states in ^{16}O as a function of ϵ_x.

This procedure introduces, besides the quoted errors, a further uncertainty on the a_k coefficients which can be estimated around 5% for a_1, a_2, and a_3 but which increases up to 40% for a_4.

A quantitative evaluation of the expansion coefficients for the main transitions to the 6.13+6.92 MeV and 12.6+13.1 MeV levels is reported in Fig. 6. In both cases the angular distribution shows dominant $E1$ absorption, responsible for the larger a_2 values, with non-negligible ($E1$,$E2$) interference terms, contained in the a_1 and a_3 coefficient. Pronounced $E2$ resonances in the excitation energy region between 30 and 40 MeV have been, in fact, recently observed in the ^{12}C(α,γ_x) cross section.[25] For the 8.87–9.63 MeV levels only the total cross section (Fig. 7) has been measured with acceptable precision, while the peak around $\epsilon_x = 10.9$–11.6 MeV was always too weak for a reliable background subtraction.

In Fig. 7 the total capture cross sections $\sigma_T = 4\pi A_0$ to the 1p-1h ($1p_{1/2}^{-1}$) residual states of ^{16}O as a function of the excitation energy are displayed. The most interesting feature of these data is the systematic existence of resonances in each channel; this effect has already been observed by different groups[4,5] in ^{12}C and a simple model has been suggested[6,4] to describe each resonance as a giant resonance built on the corresponding residual state.

According to this suggestion the shift energy ΔE_γ of each resonance with respect to its background level should be approximately constant and comparable to the centroid energy of the giant dipole resonance; the resonances reported in Fig. 7 are instead all in the 33–35 MeV interval. Nevertheless, one should point out that in ^{12}C a simple relation holds[8] between the average energy

$$\langle E \rangle = \int E_x \sigma_{\gamma_x}(E_x) dE_x / \sigma_{\text{int}}$$

and the residual state energy ϵ_x, namely [see Fig. 8(a)]

$$\Delta E_\gamma = \langle E \rangle - \epsilon_x \simeq \text{const} ,$$

where

$$\sigma_{\text{int}} = \int \sigma_{\gamma_x}(E_x) dE_x$$

and $\sigma_{\gamma_x} = 4\pi A_0$ is the total cross section for each pγ_x transition reported in Fig. 7. Unfortunately the fragmentary measurements[17,20] of the low energy capture cross section to excited states, presently available in ^{16}O, make the evaluation of $\langle E \rangle$ in this nucleus more problematic. The average energy shift ΔE_γ, displayed for each residual state energy ϵ_x in ^{16}O in Fig. 8, has been calculated above 17.5 MeV for the pγ_0 using the available 90° low energy data[20] for the p,γ_{1+2} transition; for the remaining transitions, where low energy points are missing, our data only provide an upper limit. The corresponding integrated cross

sections up to 50 MeV are plotted in Fig. 8(b); the integrated detail balanced cross sections for the inverse γ_xp transition can be obtained by multiplying the data points in Fig. 8(b) at $\epsilon_x = 6.5$, 9.3, and 12.8 MeV by the factor $K_x = 117.$, 106.6, and 148, respectively.

Complete measurements of low energy capture cross sections are definitely required for conclusions, but for the moment the present results on ^{16}O seem still compatible with a schematic model of giant dipole resonances built on excited states where each resonance has an approximately constant centroid energy shift but a typical structure. This assumption is supported by the dominant $E1$ character of the angular distribution, where the relevant interference effects also confirm the existence of a complex structure.

[1]G. Ricco, in *Lecture Notes in Physics 61, Photonuclear Reactions I* (Springer, Berlin, 1977), p. 223.

[2]M. Gary and H. Hebach, Phys. Rep. 72, 1 (1981).

[3]M. A. Kovash, S. L. Blatt, R. N. Boyd, T. R. Donoghue, H. J. Hausman, and A. Bacher, Phys. Rev. Lett. 42, 400 (1979).

[4]H. R. Weller, H. Hasan, S. Manglos, G. Mitev, N. R. Roberson, S. L. Blatt, H. J. Hausman, R. G. Seyler, R. N. Boyd, T. R. Donoghue, M. A. Kovash, A. D. Bacher, and C. C. Foster, Phys. Rev. C 25, 2921 (1982).

[5]M. Anghinolfi, P. Corvisiero, G. Ricco, M. Taiuti, and A. Zucchiatti, Nucl. Phys. A399, 66 (1983).

[6]J. T. Londergan and L. D. Ludeking, Phys. Rev. C 25, 1722 (1982); S. F. Tsai and J. T. Londergan, Phys. Rev. Lett. 43, 576 (1979).

[7]R. J. Philpott and D. Halderson, Nucl. Phys. A375, 169 (1982).

[8]M. Anghinolfi, P. Corvisiero, M. Guarnone, G. Ricco, M. Sanzone, and A. Zucchiatti, Nuovo Cimento (to be published).

[9]K. A. Snover, Invited talk at the International Conference on Giant Multipole Resonances, Mainz, 1982.

[10]M. Anghinolfi, P. Corvisiero, E. Durante, M. Guarnone, M. Taiuti, and A. Zucchiatti, Nuovo Cimento (to be published).

[11]P. Corvisiero, M. Taiuti, A. Zucchiatti, and M. Anghinolfi, Nucl. Instrum. Methods 185, 291 (1981).

[12]M. Taiuti, M. Anghinolfi, P. Corvisiero, G. Ricco, and A. Zucchiatti, Nucl. Instrum. Methods (to be published).

[13]D. J. Findlay and R. O. Owens, Nucl. Phys. A279, 385 (1977).

[14]M. Cavinato, M. Marangoni, P. Ottaviani, and A. M. Saruis, Nucl. Phys. A373, 445 (1982); M. Cavinato, M. Marangoni, and A. M. Saruis, Nuovo Cimento (to be published).

[15]F. W. K. Firk, Annu. Rev. Nucl. Sci. 20, 39 (1970).

[16]A. M. Saruis (private communication).

[17]W. J. O'Connel and S. S. Hanna, Phys. Rev. C 17, 892 (1979).

[18]H. Hebach (private communication).

[19]T. W. Phillips and R. G. Johnson, Phys. Rev. C 20, 1689 (1979).

[20]S. H. Chew, J. Lowe, J. M. Nelson, and A. R. Barnett, Nucl. Phys. A295, 241 (1979).

[21]S. Boffi, C. Giusti, and F. D. Pacati, Nucl. Phys. A359, 91 (1981).

[22]S. Boffi, Nuovo Cimento (to be published).

[23]A. Arima, G. E. Brown, H. Hyuga, and M. Ichimura, Nucl. Phys. A205, 27 (1973).

[24]B. L. Berman, R. Bergére, and P. Carlos, Phys. Rev. C 26, 304 (1982).

[25]A. M. Sandorfi, M. T. Collins, D. J. Millener, A. M. Nathan, and S. F. Le Brun, Phys. Rev. Lett. 16, 884 (1981).

[26]M. Marangoni, P. L. Ottaviani, and A. M. Saruis, Comitato Nazionale Energia Nucleare Report RT/FI(76)10, 1976.

[27]E. D. Earle and N. W. Tanner, Nucl. Phys. A95, 241 (1967).